TOXICON

Pulmonary gene expression profiling of inhaled ricin

Luis DaSilva[a],[*], Dawn Cote[a], Chad Roy[a], Mark Martinez[b], Steve Duniho[b],
M. Louise M. Pitt[a], Thomas Downey[c], Mark Dertzbaugh[d]

[a]*Toxinology and Aerobiology Division, United States Army Medical Research Institute of Infectious Diseases, Frederick, MD 21702, USA*
[b]*Pathology Division, United States Army Medical Research Institute of Infectious Diseases, Frederick, MD 21702, USA*
[c]*Partek Inc., 4 Research Park Dr., St Charles, MO 63304, USA*
[d]*Research Programs Office, United States Army Medical Research Institute of Infectious Diseases, Frederick, MD 21702, USA*

Abstract

Aerosol exposure to ricin causes irreversible pathological changes of the respiratory tract resulting in epithelial necrosis, pulmonary edema and ultimately death. The pulmonary genomic profile of BALB/c mice inhalationally exposed to a lethal dose of ricin was examined using cDNA arrays. The expression profile of 1178 mRNA species was determined for ricin-exposed lung tissue, in which 34 genes had statistically significant changes in gene expression. Transcripts identified by the assay included those that facilitate tissue healing (early growth response gene (egr)-1), regulate inflammation (interleukin (IL)-6, tristetraproline (ttp)), cell growth (c-myc, cytokine-inducible SH2-containing protein (cish)- 3), apoptosis (T-cell death associated protein (tdag)51, pim-1) and DNA repair (ephrin type A receptor 2 (ephA2)). Manipulation of these gene products may provide a means of limiting the severe lung damage occurring at the cellular level. Transcriptional activation of egr-1, cish-3, c-myc and thrombospondin (tsp)-1 was already apparent when pathological and physiological changes were observed in the lungs at 12 h postexposure. These genes may well serve as markers for ricin-induced pulmonary toxicity. Ongoing studies are evaluating this aspect of the array data and the potential of several genes for clinical intervention.
© 2003 Elsevier Science Ltd. All rights reserved.

Keywords: cDNA array; Inflammation; Lungs; Ricin

1. Introduction

Ricin is a highly toxic protein that can be easily purified in large quantities from the beans of the castor bean plant, *Ricinus communis*. The holotoxin is a 65 kDa type II ribosome-inactivating glycoprotein, which contains two polypeptide chains joined by a disulfide bond; the A chain represents the toxic moiety and the B chain represents the lectin moiety (Cushley et al., 1984). The lectin properties of the B chain allow for rapid uptake of the toxin through galactoside moieties of cell surface carbohydrates. Once inside the cell, catalytic cleavage of the 28 S ribosomal RNA by the A chain occurs, resulting in inhibition of protein synthesis and ultimately cell death. The severity of ricin toxicity is dependent upon the dose of the toxin and the route of exposure. In rodents and non-human primates, inhalation of small-particle aerosols containing ricin cause airway and pulmonary lesions resulting in respiratory distress (Xu et al., 1995). If ingested, this toxin can cause severe gastrointestinal toxicity and subsequent damage of the liver, spleen and kidneys (Rauber and Heard, 1985). When injected intramuscularly, ricin causes muscular pain, microcirculatory failure and organ failure (Balint, 2000; Baluna et al., 1996; Fodstad et al., 1984). Due to ricin's high toxicity, this toxin has been used as an immunotherapeutic agent in cancer treatment (Longo et al., 2000). Ricin also meets the criteria for an agent of warfare (Crompton and Gall, 1980); therefore, it is classified as a schedule 1 threat agent by the Chemical Weapons Convention (Hay, 2000). Ricin can rapidly enter the cell and inhibit protein synthesis, leading

---

* Corresponding author. Tel.: +1-301-619-4603; fax: +1-301-619-2348.
E-mail address: luis.dasilva@amedd.army.mil (L. DaSilva).

Report Documentation Page

Public reporting burden for the collection of information is estimated to average 1 hour per response, including the time for reviewing instructions, searching existing data sources, gathering and maintaining the data needed, and completing and reviewing the collection of information. Send comments regarding this burden estimate or any other aspect of this collection of information, including suggestions for reducing this burden, to Washington Headquarters Services, Directorate for Information Operations and Reports, 1215 Jefferson Davis Highway, Suite 1204, Arlington VA 22202-4302. Respondents should be aware that notwithstanding any other provision of law, no person shall be subject to a penalty for failing to comply with a collection of information if it does not display a currently valid OMB control number.

1. REPORT DATE **01 FEB 2003**	2. REPORT TYPE **N/A**	3. DATES COVERED **-**

4. TITLE AND SUBTITLE **Pulmonary gene expression profiling of inhaled ricin, Toxicon 41:813-822**	5a. CONTRACT NUMBER
	5b. GRANT NUMBER
	5c. PROGRAM ELEMENT NUMBER
6. AUTHOR(S) **DaSilva, L Cote, D Roy, C Martinez, M Duniho, S Pitt, ML Downey, T Dertzbaugh, M**	5d. PROJECT NUMBER
	5e. TASK NUMBER
	5f. WORK UNIT NUMBER

7. PERFORMING ORGANIZATION NAME(S) AND ADDRESS(ES) **United States Army Medical Research Institute of Infectious Diseases, Fort Detrick, Maryland**	8. PERFORMING ORGANIZATION REPORT NUMBER

9. SPONSORING/MONITORING AGENCY NAME(S) AND ADDRESS(ES)	10. SPONSOR/MONITOR'S ACRONYM(S)
	11. SPONSOR/MONITOR'S REPORT NUMBER(S)

12. DISTRIBUTION/AVAILABILITY STATEMENT
Approved for public release, distribution unlimited

13. SUPPLEMENTARY NOTES
The original document contains color images.

14. ABSTRACT
Aerosol exposure to ricin causes irreversible pathological changes of the respiratory tract resulting in epithelial necrosis, pulmonary edema and ultimately death. The pulmonary genomic profile of BALB/c mice inhalationally exposed to a lethal dose of ricin was examined using cDNA arrays. The expression profile of 1178 mRNA species was determined for ricin-exposed lung tissue, in which 34 genes had statistically significant changes in gene expression. Transcripts identified by the assay included those that facilitate tissue healing (early growth response gene (egr)-1), regulate inflammation (interleukin (IL)-6, tristetraproline (ttp)), cell growth (c-myc, cytokine-inducible SH2-containing protein (cish)- 3), apoptosis (T-cell death associated protein (tdag)51, pim-1) and DNA repair (ephrin type A receptor 2 (ephA2)). Manipulation of these gene products may provide a means of limiting the severe lung damage occurring at the cellular level. Transcriptional activation of egr-1, cish-3, c-myc and thrombospondin (tsp)-1 was already apparent when pathological and physiological changes were observed in the lungs at 12 h postexposure. These genes may well serve as markers for ricin-induced pulmonary toxicity. Ongoing studies are evaluating this aspect of the array data and the potential of several genes for clinical intervention.

15. SUBJECT TERMS
Ricin, aerosol, inhaled dose, pulmonary gene expression, cDNA array, inflammation, lungs

16. SECURITY CLASSIFICATION OF:			17. LIMITATION OF ABSTRACT	18. NUMBER OF PAGES	19a. NAME OF RESPONSIBLE PERSON
a. REPORT **unclassified**	b. ABSTRACT **unclassified**	c. THIS PAGE **unclassified**	**SAR**	**10**	

inevitably to cell death. Its high catalytic efficiency poses a major obstacle for the development of effective therapeutic strategies. The cell responds to ricin toxicity by activating its defensive mechanisms such as evoking inflammatory processes, altering protein trafficking, cell differentiation and turning on apoptotic signals (Day et al., 2001; Elson et al., 2001; Griffiths et al., 1999; Hu et al., 2001). Relatively little is known of the role that these or any other gene regulatory circuits may play in the intoxication process initiated by ricin. However, the knowledge of such intricate circuits is critical for the development of effective prophylactic and therapeutic countermeasures to ricin. To gain insight into such mechanisms, we used cDNA array technology. With the help of this methodology, we obtained the global gene expression profile for the lungs of BALB/c mice after exposure to aerosolized ricin. This differential genomic profile correlated with the pathological changes observed in the lungs, with the appearance of indicators of inflammation, and an increase of macrophages in alveolar spaces. The data can be exploitable for improved therapeutic and even preventive strategies against ricin.

2. Materials and methods

Animals and reagents. BALB/c mice were purchased from the National Cancer Institute Animal Production Area (Frederick, MD). Ricin holotoxin was purchased from Inland Laboratories, Austin, TX.

Exposure to aerosolized ricin. BALB/c mice were divided in two groups containing a minimum of 21 mice each. One group received whole-body aerosol exposure to ricin at a dose of approximately 1 aerosol LD_{50} (14 μg/kg) and the second group received aerosolized saline. The mice were exposed to ricin or saline by aerosol in a whole-body exposure chamber within a Class III safety cabinet. The aerosols were sized using an Aerodynamic Particle Sizer (APS 3320, TSI Instruments, St Paul, MN) and indicated a mass median aerodynamic diameter of 0.9 μm (geometric standard deviation $= 1.4$). The test atmosphere was continuously sampled via impingement to determine aerosol concentration. Ricin concentrations from impinger samples were measured by protein assay (Pierce, MicroBCA, Rockford, IL). The ricin dose was calculated from the empirically determined aerosol chamber and the estimated rodent minute volume based on Guyton's formula and the arithmetic mean of intergroup mouse weights. Animals were exposed to the aerosol for 10 min. At the indicated time point after aerosol exposure (1, 4, 12, 24, 48, 96 and 192 h), a minimum of three mice per group received a lethal dose of CO_2 and their lungs were removed for isolation of total RNA or histopathology analysis.

Processing ricin-exposed BALB/c lung tissue for cDNA array analysis. Total RNA was isolated from lung tissue of BALB/c mice exposed to aerosolized ricin or saline alone.

The lungs were homogenized and RNA extracted using the RNeasy protect kit (QIAGEN, Valencia, CA). The RNA was digested with DNase during the RNA purification process using QIAGEN's RNase-free DNase set.

cDNA array analysis of ricin-exposed BALB/c lung tissue. Radiolabeled cDNA array probes were generated from purified lung RNA (10 μg) from saline- or ricin-exposed mice. The cDNA array probes were hybridized to the CLONTECH Mouse 1.2 arrays for 16 h at 70 °C. Probe preparation, hybridization and high-stringency washes were performed according to the manufacturer's specifications (Atlas Pure Total RNA Labeling System, CLONTECH, Palo Alto, CA). The array was exposed for 3–7 days and scanned using the BioRad Molecular Imager FX (Hercules, CA). Array images were processed using ArrayVision software (Imaging Research, St. Catherines, Canada) and the pixel intensity of each spot on the array was expressed as artifact-removed volume (AR VOL). AR VOL represents the pixel density value multiplied by the area of the spot. Image artifacts in the spots were corrected by excluding pixel densities exceeding 3.0 median of absolute deviations and replacing the values with estimated values derived by interpolation from neighboring pixels in the spot. Statistical evaluation of the cDNA array data was performed using Partek Pro 5.0 and Partek Infer software packages (St Charles, MO). In the statistical analysis, sample-to-sample scaling was performed to the cDNA array data (AR VOL) using the percentile mean scaling method followed by $\log_2$ transformation of the scaled data (Partek Pro 5.0, St Charles, MO). Requests for raw data should be submitted to the corresponding author.

Gene-specific RT-PCR analysis. Semi-quantitative gene-specific RT-PCR was performed to confirm the cDNA array data. RNA (1 μg) was reverse transcribed using the Advantage RT-for-PCR kit (CLONTECH, Palo Alto, CA) and random hexamer primers. Further amplification of the cDNA was accomplished by AmpliTaq in a 30-cycle PCR. The PCR cycling conditions for denaturing, annealing and extension were 45 s at 94 °C, 45 s at 60 °C and 2 min at 72 °C, respectively. The PCR fragments were resolved on a 1.8% agarose gel. The DNA bands were measured by GeneTools software (Syngene, Frederick, MD), assigning a quantity of 100 for the pixel intensity of the co-amplified β-actin DNA. The sense and antisense RT-PCR primer sequences were obtained from Atlas Nylon RT-PCR sequence database (CLONTECH, Palo Alto, CA).

Histopathology analysis of ricin-exposed BALB/c lung tissue. Lungs from BALB/c mice were immersion-fixed for 48–72 h in 10% neutral buffered formalin for histology evaluation. Fixed tissues were processed in an automatic tissue processor, embedded in paraffin blocks, sectioned at 5–6 μm on a standard rotary microtome, and mounted on glass microslides for automated staining with hematoxylin and eosin in a Sakura DRS 601 Slide Stainer (Sakura Finetek USA, Inc., Torrance, CA). To detect pulmonary alveolar macrophages, replicate sections of formalin-fixed,

paraffin-embedded lung specimens were assayed for histiocytic lysozyme using an alkaline phosphatase (AP) immunohistochemistry kit (AP IHC, Envision System, DAKO Corporation, Carpinteria, CA). The rabbit poly-clonal antiserum generated against lysozyme (DAKO Corporation, Carpinteria, CA) was used as the primary antibody (1:500 dilution) and incubated for 16 h at room temperature in the presence of antimouse and antirabbit polymer AP (DAKO Corporation, Carpinteria, CA), and naphthol AS-BI phosphate/hexazotized new fuchsin (His-toMark® RED Phosphatase System, Kirkegaard and Perry Laboratories, Gaithersburg, MD).

Protein assay. BCA protein assay (Pierce, Rockford, IL) was performed in the lung lavage samples. Each mouse was subjected to three bronchoalveolar lavages of 1 ml Hank's balanced salt solution (HBSS) each. The lavages were pooled and an aliquot taken for determination of protein amounts in the lavage liquid.

Body weight measurements. Each BALB/c mouse was weighed at 1, 4, 12, 24, 48, 96 and 192 h postexposure.

3. Results

3.1. Array-to-array scaling and normalization of expression data

In order to evaluate the host pulmonary responses to inhaled ricin, we determined the gene expression profile of the lungs of BALB/c after exposure to aerosolized ricin at several time intervals. The signals from the mouse arrays for the ricin-exposed lungs were to be compared to those exposed to saline. However, we observed that the unprocessed AR VOL gene expression measures had significantly different distributions from array to array. For this reason, we performed array-to-array scaling. For each array, we first subtracted the minimum value for that array resulting in each array having a minimum expression value of 0. Next, we computed the trimmed mean of the lower 50% of the expression values on each array. These trimmed means were used to perform a linear rescaling of all arrays to a single reference (saline 1 h exposure array). The result is that all arrays now have the same mean in the lower 50%. After performing the array-to-array scaling, we applied a $\log_2$ transformation to make the distributions more normally distributed. The result of array-to-array scaling and normalization is summarized by Fig. 1. Note that each array has a distribution which is relatively normal and that the distributions from all the arrays are comparable. The scaled and normalized AR VOL expression values were now capable of providing reliable array-to-array comparisons. The statistically significant changes in gene expression were determined by performing unbalanced two-way analysis of variance (ANOVA) on each gene to test for statistically significant differences between ricin and saline and also between different time points. A Dunn-Sidak correction was applied to the p-values to adjust for the multiple tests run on the genes.
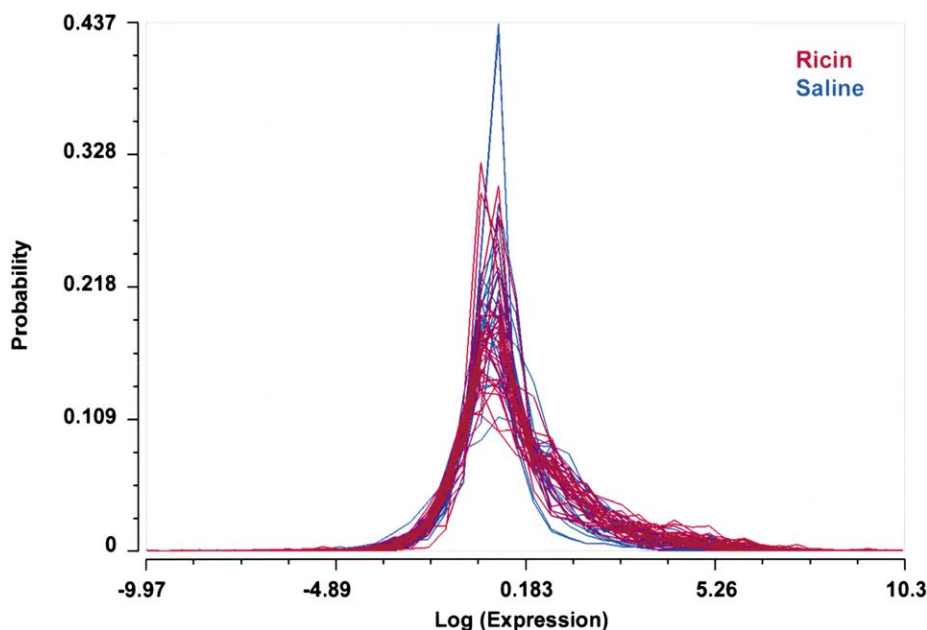

Fig. 1. Probability distribution of gene expression of the 49 cDNA arrays. After $\log_2$ transformation for normalization and array-to-array scaling of the data using Partek Pro software, the distributions of the 49 arrays were relatively normal allowing the genes on different arrays to be compared. Each line represents the distribution of one array corresponding to BALB/c mice that have been exposed to either aerosolized ricin or saline. Ricin is shown in red and saline in blue.

The list of genes differentially expressed between ricin and saline is summarized in Table 1 (genes that have a corrected *p*-value ≤ 0.05). The genes were grouped by their potential roles in inflammatory processes in the lungs.

In Table 1, the mean AR VOL is reported for each gene for the ricin and saline arrays. This value corresponds to the mean of the normalized AR VOL, combining all time points, without log transformation. The data revealed that

Table 1
Differential gene expression detected by cDNA array analysis

Gene name	Ricin mean AR VOL	Saline mean AR VOL	*p*-Value (ricin/saline)	Dunn-Sidak corrected *p*-value (ricin/saline)
Apoptosis				
Anti-proliferative B-cell translocation gene 2 (BTG2)	13.14	5.31	4.62×10^{-6}	5.44×10^{-3}
Pim1 proto-oncogene	4.76	1.88	4.74×10^{-7}	5.60×10^{-4}
Thrombospondin 1 precursor (THBS1; TSP1)	13.65	2.67	1.88×10^{-9}	2.23×10^{-6}
T-cell death-associated protein (TDAG51)	7.84	1.86	4.44×10^{-9}	5.25×10^{-6}
Cell growth and differentiation				
C-fos proto-oncogene	3.22	1.18	2.05×10^{-6}	2.42×10^{-3}
C-myc proto-oncogene	5.36	1.03	6.08×10^{-11}	7.19×10^{-8}
Cytokine inducible SH2-containing protein 3 (CISH3)	3.81	1.06	5.19×10^{-9}	6.13×10^{-6}
Fos-related antigen 2 (FRA2)	4.06	1.65	1.86×10^{-7}	2.19×10^{-4}
Inhibin beta-B precursor	1.75	1.02	1.61×10^{-6}	1.90×10^{-3}
Macrophage colony stimulating factor 1 precursor (MCSF)	3.09	0.98	3.74×10^{-9}	4.42×10^{-6}
MAP kinase-activated protein kinase (MAPKAPK-2)	2.49	1.36	1.92×10^{-5}	2.24×10^{-2}
Serine protease inhibitor 2-2 (SPI2-2)	3.06	0.85	5.34×10^{-7}	6.31×10^{-4}
Stimulated by Retinoic Acid Protein 14 (STRA14)	6.30	1.88	2.02×10^{-8}	2.39×10^{-5}
Cellular matrix				
Fibronectin 1 precursor (FN1)	47.89	14.73	4.52×10^{-5}	5.20×10^{-2}
Type I cytoskeletal keratin 18 (KRT1-18)	2.23	1.15	3.88×10^{-7}	4.59×10^{-4}
DNA repair				
Ephrin type A receptor 2 (EPHA2)	1.43	0.84	1.68×10^{-5}	1.97×10^{-2}
Inflammation and cell trafficking				
CD14 monocyte differentiation antigen precursor	8.40	2.15	1.39×10^{-9}	1.65×10^{-6}
Intercellular adhesion molecule 1 precursor (ICAM1)	18.44	4.69	5.24×10^{-9}	6.18×10^{-6}
Interleukin-6 precursor (IL-6)	1.22	0.43	1.80×10^{-8}	2.13×10^{-5}
Macrophage inflamatory protein 1 beta (Act 2)	1.22	0.48	4.15×10^{-6}	4.89×10^{-3}
Monocyte chemoattractant protein 3	2.57	0.79	7.42×10^{-8}	8.76×10^{-5}
Tristetraproline (TTP)	3.53	1.22	4.47×10^{-6}	5.27×10^{-3}
Integrin alpha 7	1.47	0.83	2.84×10^{-5}	3.30×10^{-2}
Cell surface glycoprotein MAC-1 alpha subunit precursor	1.72	0.89	3.61×10^{-5}	4.17×10^{-2}
Lung injury/healing				
Early growth response protein 1 (EGR1)	32.78	2.51	7.39×10^{-17}	1.31×10^{-13}
NFKB signaling				
I-kappa B alpha subunit (IKB alpha)	8.60	2.18	6.64×10^{-11}	7.85×10^{-8}
Nuclear factor of kappa light chain protein enhancer in B-cells inhibitor alpha (IKB-beta)	2.75	1.25	4.76×10^{-8}	5.62×10^{-5}
Transcription factor relB	1.54	0.74	3.06×10^{-7}	3.61×10^{-4}
Tumor necrosis factor alpha-induced protein 3 (TNFAIP3)	1.36	0.70	2.37×10^{-6}	2.79×10^{-3}
Transcription factor				
Activating transcription factor 4 (mATF4)	0.94	0.63	3.24×10^{-5}	3.76×10^{-2}
Albumin D box-binding protein	4.04	1.34	2.50×10^{-7}	2.96×10^{-4}
cAMP-dependent transcription factor 3 (ATF3)	1.31	0.56	2.28×10^{-11}	2.69×10^{-8}
Early growth response protein 2 (EGR2)	1.17	0.61	2.48×10^{-6}	2.93×10^{-3}
Interferon regulatory factor 1 (IRF1)	14.60	5.50	7.07×10^{-8}	8.35×10^{-5}

all 34 statistically significant transcripts had higher expression levels in the lungs exposed to ricin than to saline (Table 1).

3.2. Changes in pulmonary gene expression after ricin inhalation

As shown in Table 1, ricin transcriptionally activated a number of inflammatory mediators, including il-6, serine protease inhibitor (spi) 2.2, interferon regulatory factor (irf)-1 and several members of the nuclear factor (NF)-kappa B/rel family of transcription factors (nuclear factor of kappa

light chain protein enhancer in B-cells inhibitor alpha (NFKBIA), I-kappa B and tumor necrosis factor alpha-induced protein (tnfaip)-3. The enhanced transcriptions of macrophage colony stimulating factor 1 (mcsf), cd14, monocyte chemoattractant protein (mcp)-3, macrophage inflammatory protein (mip)-1β and intercellular adhesion molecule (icam)-1 were also observed and possibly reflect sustained phagocytic activity and transendothelial trafficking of immune cells into the lungs due to ricin cytotoxicity. By examining the results in Table 1, we observed the induction of cell death regulatory factors, such as the anti-proliferative B-cell translocation gene (btg)2, tdag51, the kinase pim1
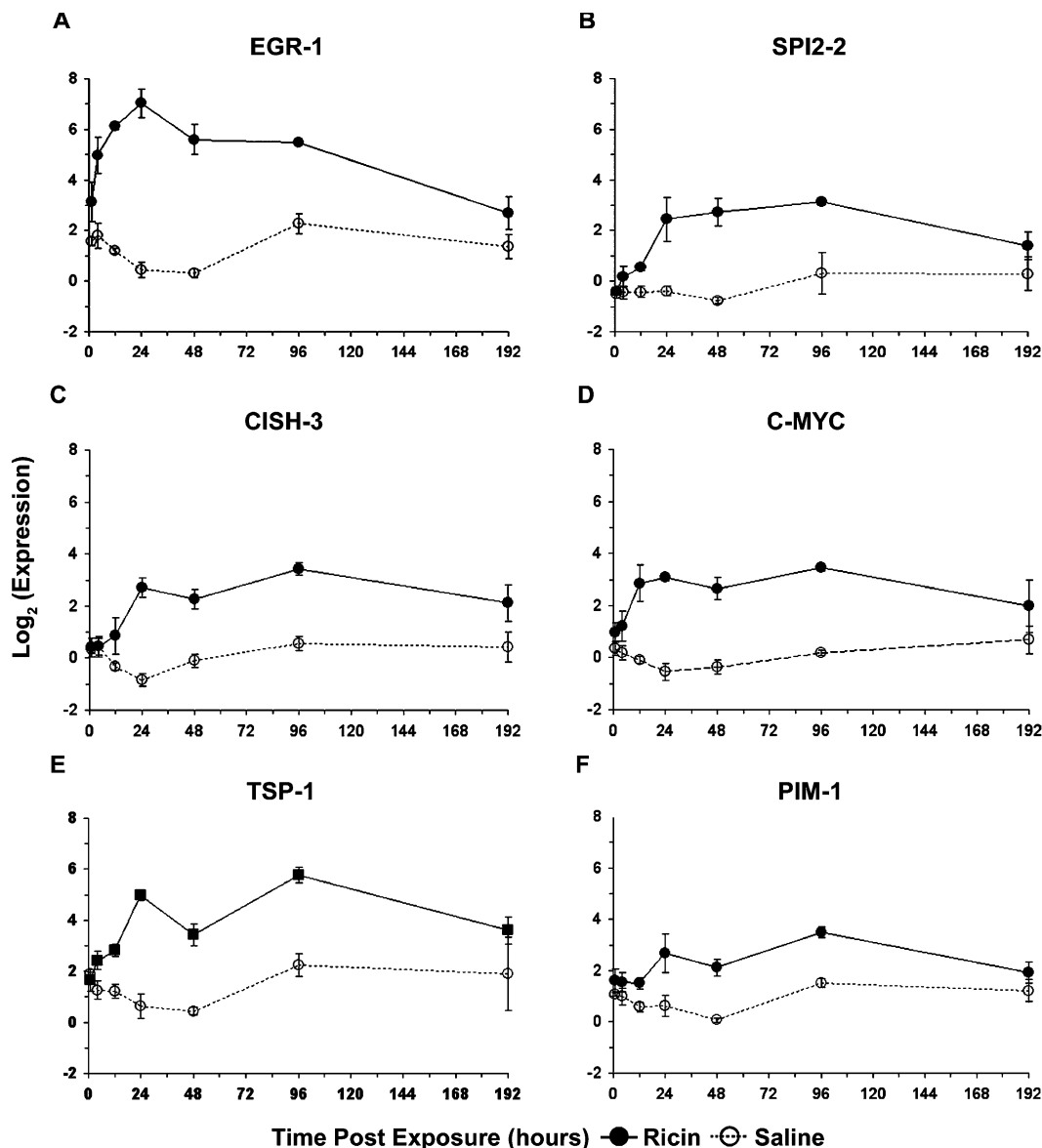

Fig. 2. Identification of ricin-responsive genes in the lungs by temporal cDNA array analysis. The graphs display normalized AR VOLs for the genes (A) egr-1, (B) spi2.2, (C) cish-3, (D) c-myc, (E) tsp-1, and (F) pim-1. The AR VOLs were collected from the cDNA array experiments at 1, 4, 12, 24, 48, 96 and 192 hr post exposure to aerosolized ricin (●) or saline (○).

and tsp1, after exposure to aerosolized ricin (Table 1). A comparison of the results also demonstrate elevated levels of ttp and egr1 transcripts, which may indicate that these transcripts help BALB/c mice maintain the balance of inflammatory and reparative responses in the intoxicated lungs (Crawford et al., 1998). In addition, eph A2, which is normally activated in response to DNA damage, was elevated in the presence of ricin in the lungs as well as the extracellular matrix proteins, fibronectin and type 1 cytoskeletal keratin 18 (Table 1). Upregulation of the following genes were also noted: ATF family members,

albumin D-box binding protein and stimulated by retinoic acid protein (stra) 14; however, the significance of this upregulation is not clear at this time. The data reported herein should greatly contribute to the understanding of the host's pulmonary responses to ricin.

3.3. Temporal regulation of RNA transcripts by ricin

To determine the sequence of molecular events that occur in the lungs after ricin inhalation, the gene expression profile was monitored over 192 h. Fig. 2 shows the changes
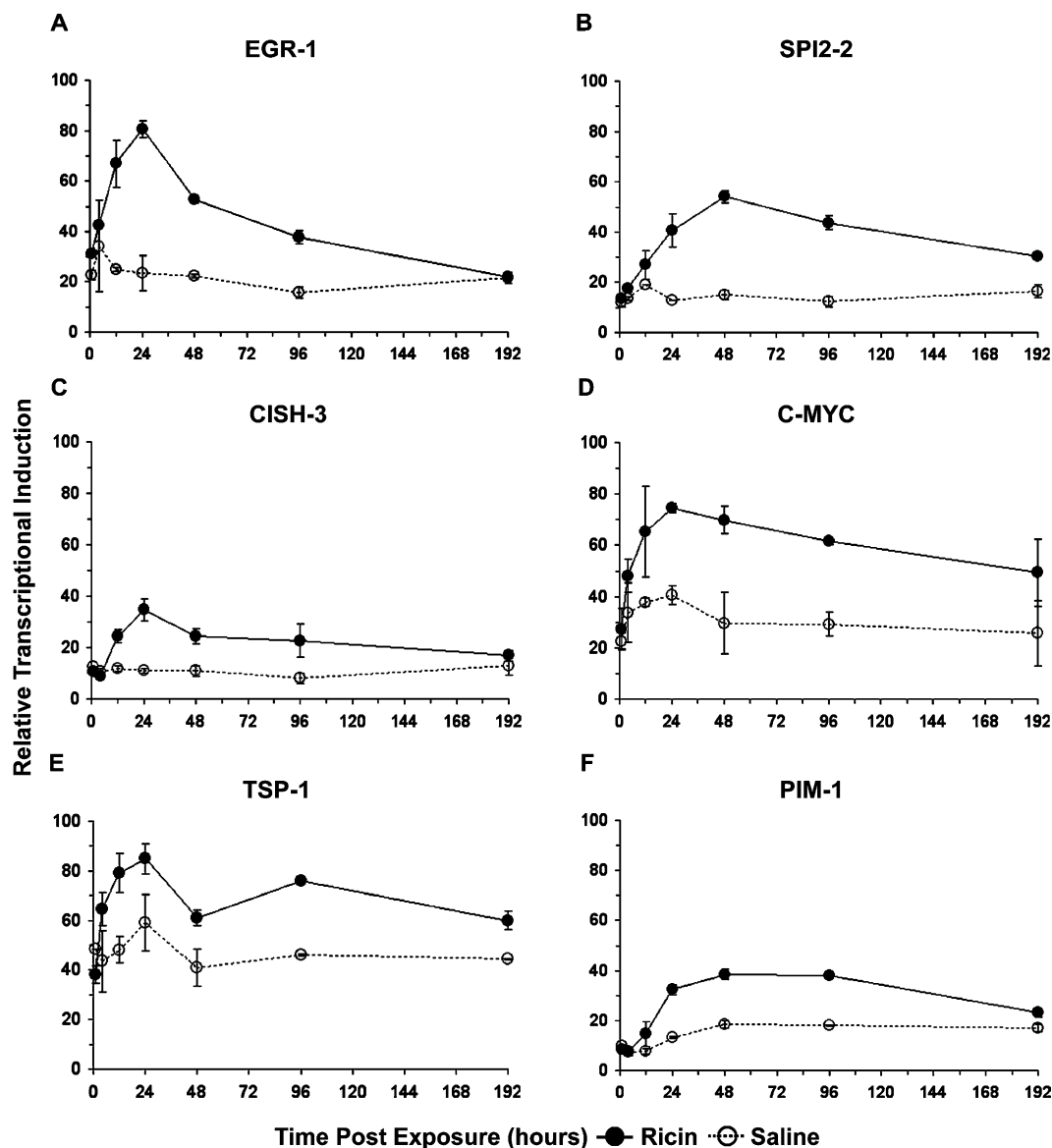

Fig. 3. Time course of differentially expressed genes in the lungs after exposure to inhaled saline or ricin. Total RNA was isolated from the lungs of BALB/c mice at 1, 4, 12, 24, 48, 96 and 192 h after exposure to either aerosolized ricin (●) or saline (○). Semi-quantitative RT-PCR was performed in those samples for the genes (A) egr-1, (B) spi2.2, (C) cish-3, (D) c-myc, (E) tsp-1, and (F) pim-1. To determine the relative induction levels for each gene, a quantity of 100 was assigned for the pixel intensity of the co-amplified β-actin DNA in the RT-PCR reaction.

in pulmonary gene expression occurring during this period for six genes of the array (egr-1, spi2.2, cish-3, c-myc, tsp-1 and pim-1). We chose these genes for their recognized involvement in major regulatory functions that may be relevant for ricin research (Braddock, 2001; Berry et al., 1999; Carballo et al., 2000; Egwuagu et al., 2002; Lawler et al., 1998; Nosaka et al., 1999; Zajac-Kaye, 2001). The cDNA array data (Fig. 2 and Table 1) demonstrate that mice exposed to aerosolized ricin had higher expression levels of egr-1, spi2.2, cish-3, c-myc, tsp-1 and pim-1 in their lungs than those exposed to aerosolized saline. RT-PCR analysis was performed subsequently to confirm the differential expression of these genes (Fig. 3). The RT-PCR results reflected very closely those obtained by cDNA array analysis (compare Figs. 2 and 3). In both cases, egr1 (Fig. 2a and 3a) was the first transcript to be induced in the lungs by aerosolized ricin. This transcript was observed as early as 1 h post ricin exposure. Because egr-1 has been associated with tissue injury and reparative processes, our data indicate that these events may be initiated as early as 1 hr in the ricin-intoxicated lungs. Egr-1 expression peaked at 24 h, decreasing progressively to near background levels by 192 h (Figs. 2a and 3a). Upregulation of the spi2.2 transcript 24 h post ricin exposure may reflect ongoing inflammatory responses in the lungs caused by this toxin (Figs. 2b and 3b). The growth-regulatory factors cish-3 and c-myc were upregulated by 24 h and remained activated for the duration of the experiment (192 h) (Figs. 2c and d and 3c and d). Similarly, the apoptotic genes, tsp-1 and pim-1, peaked at 24 h and remained upregulated for the remainder of the experiment (Figs. 2e and f and 3e and f). The temporal analysis of these six transcripts represents a first, significant step in establishing pathway relationships among the differentially expressed genes in ricin-intoxicated lungs.
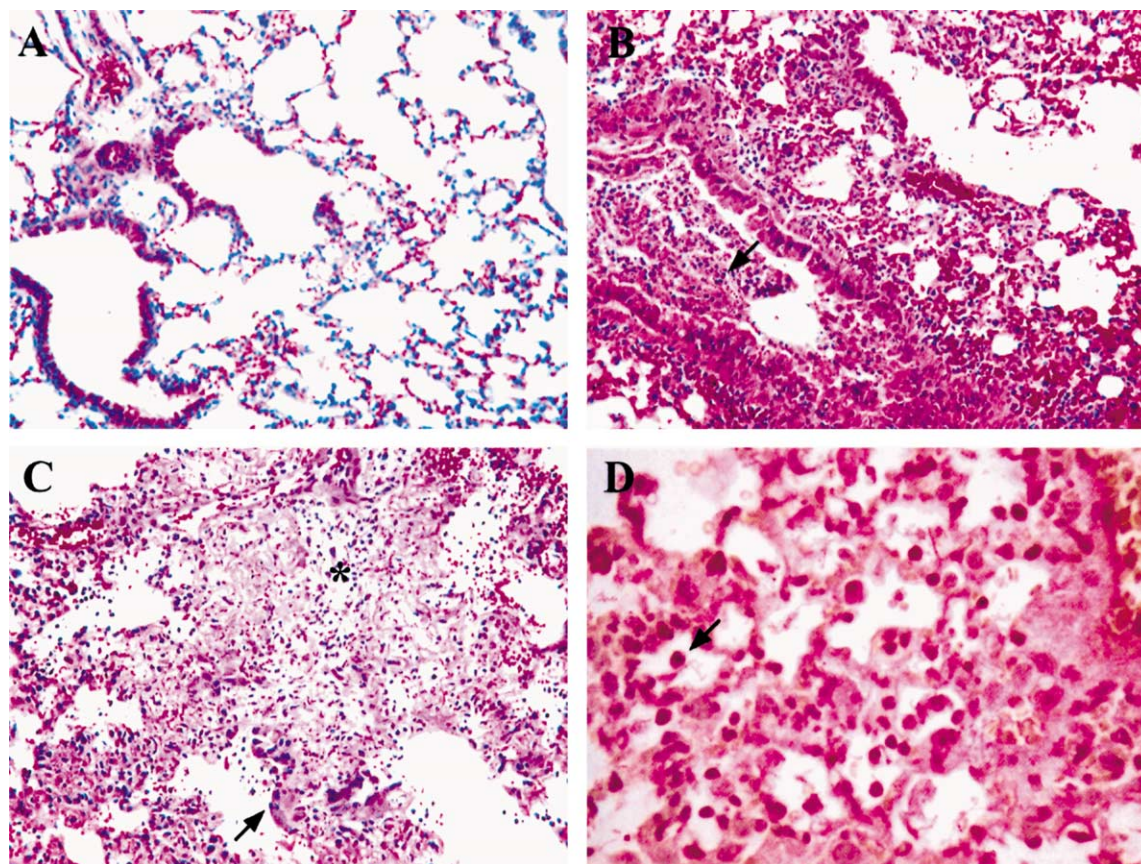

Fig. 4. Histopathologic analysis of BALB/c mouse lung tissue after exposure to aerosolized ricin. (A) No significant morphological changes were observed in the lungs up to 4 h post ricin exposure (200 ×). (B) Staining of lung tissue with hematoxylin and eosin revealed thickening of alveolar septa and perivascular areas with a large number of inflammatory cells, particularly neutrophils, in the interstitial areas and filling airways at 24 h postexposure (arrow) (200 ×). (C) At 96 h, thickening of the interstitium with fibroplasia and edema was noted (asterisk) and signs of reparative responses with type-2 pneumocyte hyperplasia were evident (arrow) (200 ×). (D) Progressively, over 96 h, we observed a moderate increase in the number of macrophages in alveolar spaces by anti-lysozyme immunoreactivity (arrow) (400 ×).

3.4. Histopathologic changes in the lungs

The histological pulmonary profile was determined for BALB/c mice after ricin or saline inhalation (Fig. 4). The histological changes were monitored at varied time points (1, 4, 12, 24, 48, 96 and 192 h) postchallenge. No significant inflammatory or toxic effects were observed in animals exposed to aerosolized saline for the entire duration of the experiment (results not shown). The lung morphology in mice was essentially normal for the first 4 h post ricin challenge (Fig. 4a). However, by 12 h post ricin challenge, predominant microscopic features of the pulmonary lesions in ricin-exposed mice were visible and were conducive of an initial, lethal injury involving pneumocytes and possibly alveolar macrophages, after which a reparative phase followed. The initial injury was characterized by thickening of the alveolar septa and influx of inflammatory cells, predominantly neutrophils (data not shown). At 24 h postexposure, necrosis of pneumocytes was prominent and we noted acute inflammation, characterized by the presence of neutrophils (Fig. 4b). These features persisted through the 48 h time point, and by 96 h, type-2 pneumocyte hyperplasia, pulmonary edema, bronchiolar epithelial reactivity, peribronchovascular fibroplasia and a further increase in the number of neutrophils were present (Fig. 4c). To confirm the presence of alveolar macrophages during the intoxication process, immunohistochemical labeling for lysozyme activity was performed in the lung tissues. Immunostaining of the lung tissue identified a discrete but progressive accumulation of macrophages in the alveolar region (Fig. 4d). The histological lesions observed in these mice are consistent with an aerosolized ricin exposure, and generally represent the temporal progression of acute pulmonary toxicity described in other animals exposed to ricin via aerosol (Poli et al., 1996; Wilhelmsen and Pitt, 1996).

3.5. Physiological changes in the lungs due to ricin toxicity

The effects of ricin toxicity were investigated to determine whether the physiological changes identified correlated with transcriptional induction observed in the intoxicated lungs. Because an increase in total protein in bronchoalveolar lavages (BAL) indicates pulmonary inflammation, the BAL protein concentration was determined for the BALB/c mice exposed to the toxin. We noted an increase in BAL protein in BALB/c mice exposed to aerosolized ricin when compared to animals exposed by inhalation to saline (Fig. 5a). BAL protein levels remained elevated for the remaining period of the observation in the ricin group (192 h, Fig. 5a). Another physiological parameter monitored was the total body weight loss; it is known that ricin intoxicated animals suffer from significant weight loss (Wilhelmsen and Pitt, 1996). Indeed, a reduction of approximately 25% of the original weight was observed for BALB/c mice that inhaled ricin by 192 h. The mice that received the saline treatment maintained their original body
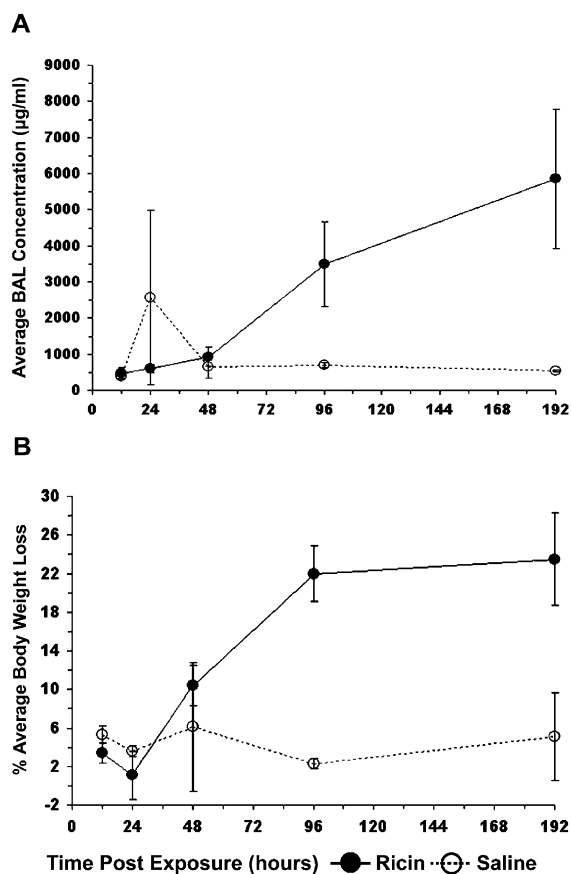

Fig. 5. Physiological changes in the lungs of BALB/c mice induced by aerosolized ricin. (A) Assay of protein content in BAL fluid after ricin exposure revealed a gradual increase in BAL protein concentration. (B) BALB/c mice showed progressive weight loss when monitored up to 192 h post ricin exposure. Significant changes in weight due to ricin exposure were noted after 48 h postexposure.

weight and appeared to be healthy throughout the observation period (Fig. 5b). Lung tissue exposed to ricin results in a progressive inflammatory response, which is consistent with the induction of known cellular mediators of inflammation identified in the cDNA array data (Table 1).

4. Discussion

The main purpose of this study was to identify potential cellular mediators of ricin toxicity in the lungs. Once identified, cellular mediators may be manipulated in a manner that would alleviate the damaging effects of ricin in the pulmonary tract, for instance, with the reduction of tissue necrosis and edematous lung injury. We set out in our genomic investigation to identify potential therapeutic targets by looking at the global gene expression profile of ricin-intoxicated lungs in BALB/c mice (Table 1).

The cDNA array results have identified a number of differentially expressed genes responsible for a variety of activities, such as regulatory functions in inflammatory processes, tissue and DNA repair, cell migration and structure, cell growth and differentiation and apoptosis. Although a few reports exist that investigate ricin's mechanism of action (Iordanov et al., 1997; Komatsu et al., 1998), more studies are needed to determine which genes are involved in the intoxication process initiated by ricin. We surmise that the earliest differentially expressed genes may play a prevalent role in ricin-mediated intoxication of the lungs. Transcripts of egr1, which has the dual capacity to promote proinflammatory gene expression in hypoxic lungs (Okada et al., 2001) and to expedite wound healing and tissue repair in other tissues (Bryant et al., 2000), is apparent as early as 1 h post ricin inhalation (Fig. 3a). Interestingly, egr1 sustained its expression levels until type II pneumocyte hyperplasia became evident at 96 h (Fig. 4c). The appearance of type II pneumocytes is indicative of active reparative processes of lung injury. The apoptotic factor tdag51, known to inhibit protein synthesis (Hinz et al., 2001), was also found to be upregulated 1 h post challenge (Table 1). A correlation between tdag51, a protein synthesis inhibitor and ricin is still unknown. Other apoptotic transcripts that were activated by ricin included tsp1, the kinase pim-1 and btg2 (Table 1). Moreover, the gene ttp was induced as early as 4 h. This gene can activate the degradative pathway for tnfα and gm-csf transcripts (Lai and Blackshear, 2001), and therefore, it may be useful in controlling the expression of inflammatory mediators.

Another element of ricin toxicity is the strong inflammatory response in the lungs. If that can be controlled, the toxicity may be reduced or even eradicated. Unpublished studies performed in our institute have suggested that the presence of alveolar macrophages in ricin intoxicated lungs of rats correlated with enhanced pulmonary toxicity (Wilhelmsen, C., personal communication). In line with this observation, our study showed that exposure to ricin was associated with the transcriptional induction of a number of cell surface inflammatory markers and chemotactic factors (Table 1). The inflammatory mediators, CD14, ICAM-1, MCP3, and MIP1β can participate in the recruitment of neutrophils or activation of tissue macrophages, which collectively could lead to acute lung injury mediated by formation of oxidants and release of proteases (Xu et al., 1995; Lukacs and Ward, 1996; Menten et al., 2001). We also detected macrophages in the alveolar region by 96 h post ricin challenge (Fig. 4c), which may be further evidence for the participation of macrophages in the intoxication process.

Induction of genes that are regulators of proliferation or cell differentiation was also noted. Increase in spi2.2, a marker of acute inflammation may be related to induction of IL-6 activity in the lungs (Berry et al., 1999). The transcription activation of these acute inflammatory factors

(Table 1) correlated with the increase in total protein in bronchoalveolar lavages (Fig. 5a) suggesting increased permeability of the air-blood barrier and cytotoxicity. Activation of cish-3 and mapkk-2 was also observed and may help clarify which intracellular pathways are most directly affected by ricin in the lungs. These pathways may affect normal lung homeostasis with the induction of fibronectin-1 and the DNA repair gene ephA2. Collectively, induction of these genes provides a better understanding of the ricin intoxication process, which needs to be taken into consideration when formulating therapeutic modalities for ricin-induced pulmonary intoxication.

During evaluation of the genomic data, one needs to consider the complexity of the lungs as a multicellular organ since cell-type specificity of the differentially expressed genes and any changes in cellular composition of the lungs may alter the global gene expression profile. Ongoing studies in our laboratory are investigating the cell-type specificity for some of these genes. Also, as more genomic information becomes available for pulmonary ricin intoxication, it can be used to generate diagnostic tools that can aid in the detection of the toxin. From our cDNA array and RT-PCR results, we observed the expression of egr1 preceding any significant histological and physiological changes (compare Fig. 3 with Figs. 4 and 5). The histological data for our animals correlate very well with those reported by Poli et al. (1996). As in our study, a loss between 20 and 30% in total body weight was observed when mice were exposed to aerosolized ricin (Poli et al., 1996). Our laboratory is further investigating this relationship between genomic, histological and physiological data. We are also determining whether the observed patterns of gene expression are unique to ricin intoxication or shared by other toxic agents, and whether these patterns are a representation of the pulmonary or systemic effects of ricin. The results described herein provide, therefore, a framework on which one can build up to develop new strategies for therapeutics, diagnostics and prevention of ricin intoxication.

References

Balint, G.A., 2000. Ultrastructural study of liver cell damage induced by ricin. Exp. Toxicol. Pathol. 52, 413–417.

Baluna, R., Sausville, E.A., Stone, M.J., Stetler-Stevenson, M.A., Uhr, J.W., Vitetta, E.S., 1996. Decreases in levels of serum fibronectin predict the severity of vascular leak syndrome in patients treated with ricin A chain-containing immunotoxins. Clin. Cancer Res. 2, 1705–1712.

Braddock, M., 2001. The transcription factor egr1: a potential drug in wound healing and tissue repair. Ann. Med. 33, 313–318.

Berry, S.A., Bergad, P.L., Stolz, A.M., Towle, H.C., Schwarzenberg, S.J., 1999. Regulation of Spi 2.1 and 2.2 gene expression after turpentine inflammation: discordant responses to IL-6. Am. J. Physiol. 276, C1374–C1382.

Bryant, M., Drew, G.M., Houston, P., Hissey, P., Campbell, C.J., Braddock, M., 2000. Tissue repair with a therapeutic transcription factor. Hum. Gene Ther. 11, 2143–2158.

Carballo, E., Lai, W.S., Blackshear, P.J., 2000. Evidence that tristetraproline is a physiological regulator of granulocyte-macrophage colony-stimulating factor messenger RNA deadenylation and stability. Blood 95, 1891–1899.

Crawford, S.E., Stellmach, V., Murphy-Ulrich, J.E., Ribeiro, S.M., Lawler, J., Hynes, R.O., Boivin, G.P., Bouck, N., 1998. Thrombospondin-1 is a major activator of TGF-beta 1 in vivo. Cell 93, 1159–1170.

Crompton, R., Gall, D., 1980. Georgi Markov—death in a pellet. Med. Leg. J. 48, 51–62.

Cushley, W., Muirhead, M.J., Silva, F., Greathouse, J., Tucker, T., Uhr, J.W., Vitetta, E.S., 1984. In vivo reconstitution of ricin-like activity from it's a and B chain subunits. Toxicon 22, 265–277.

Day, P.J., Owens, S.R., Wesche, J., Olsnes, S., Roberts, L.M., Lord, J.M., 2001. An interaction between ricin and calreticulin that may have implications for toxin trafficking. J. Biol. Chem. 276, 7202–7208.

Egwuagu, C.E., Yu, C.R., Zhang, M., Mahdi, R.M., Kim, S.J., Gery, I., 2002. Suppressors of cytokine signaling proteins are differentially expressed in Th1 and Th2 cells: implications for Th cell lineage commitment and maintenance. J. Immunol. 168, 3181–3187.

Elson, D.A., Thurston, G., Huang, L.E., Ginzinger, D.G., McDonald, D.M., Johnson, R.S., Arbeit, J.M., 2001. Induction of hypervascularity without leakage or inflammation in transgenic mice overexpressing hypoxia-inducible factor-1 alpha. Genes Dev. 15, 2520–2532.

Fodstad, O., Kvalheim, G., Godal, A., Lotsberg, J., Aamdal, S., Host, H., Pihl, A., 1984. Phase I study of the plant protein ricin. Cancer Res. 44, 862–865.

Griffiths, G.D., Phillips, G.J., Bailey, S.C., 1999. Comparison of the quality of protection elicited by toxoid and peptide liposomal vaccine formulations against ricin as assessed by markers of inflammation. Vaccine 17, 2562–2568.

Hay, A., 2000. Old dogs or new tricks: chemical warfare at the millennium. Med. Confl. Surviv. 16, 37–41.

Hinz, T., Flindt, S., Marx, A., Janssen, O., Kabelitz, D., 2001. Inhibition of protein synthesis by the T cell receptor-inducible human TDAG51 gene product. Cell. Signal. 13, 345–352.

Hu, R., Zhai, Q., Liu, W., Liu, X., 2001. An insight into the mechanisms of cytotoxicity of ricin to hepatoma cell: roles of bcl-2 family proteins, caspases, $Ca(2+)$-dependent proteases and protein kinase C. J. Cell. Biochem. 81, 583–593.

Iordanov, M.S., Pribnow, D., Magun, J.L., Dinh, T.H., Pearson, J.A., Chen, S.L., Magun, B.E., 1997. Ribotoxic stress response: activation of the stress-activated protein kinase JNK1 by inhibitors of the peptidyl transferase reaction and by sequence-specific RNA damage to the alpha-sarcin/ricin loop in the 28S rRNA. Mol. Cell. Biol. 17, 3373–3381.

Komatsu, N., Oda, T., Muramatsu, T., 1998. Involvement of both caspase-like proteases and serine proteases in apoptotic cell death induced by ricin, modeccin, diphtheria toxin, and pseudomonas toxin. J. Biochem. 124, 1038–1044.

Lai, W.S., Blackshear, P.J., 2001. Interactions of CCCH zinc finger proteins with mRNA: tristetraprolin-mediated AU-rich element-dependent mRNA degradation can occur in the absence of a poly(A) tail. J. Biol. Chem. 276, 23144–23154.

Lawler, J., Sunday, M., Thibert, V., Duquette, M., George, E.L., Rayburn, H., Hynes, R.O., 1998. Thrombospondin-1 is required for normal murine pulmonary homeostasis and its absence causes pneumonia. J. Clin. Invest. 101, 982–992.

Longo, D.L., Duffey, P.L., Gribben, J.G., Jaffe, E.S., Curti, B.D., Gause, B.L., Janik, J.E., Braman, V.M., Esseltine, D., Wilson, W.H., Kaufman, D., Wittes, R.E., Nadler, L.M., Urba, W.J., 2000. Combination chemotherapy followed by an immunotoxin (anti-B4-blocked ricin) in patients with indolent lymphoma: results of a phase II study. Cancer J. Sci. Am. 6, 135–138.

Lukacs, N.W., Ward, P.A., 1996. Inflammatory mediators, cytokines, and adhesion molecules in pulmonary inflammatory and injury. Adv. Immunol. 62, 257–305.

Menten, P., Wuyts, A., Van Damme, J., 2001. Monocyte chemoattractant protein-3 Eur. Cytokine Netw. 12, 554–560.

Nosaka, T., Kawashima, T., Misawa, K., Ikuta, K., Mui, A.L., Kitamura, T., 1999. STAT5 as a molecular regulator of proliferation, differentiation and apoptosis in hematopoietic cells. EMBO J. 18, 4754–4765.

Okada, M., Fujita, T., Sakaguchi, T., Olson, K.E., Collins, T., Stern, D.M., Yan, S.F., Pinsky, D.J., 2001. Extinguishing Egr-1-dependent inflammatory and thrombotic cascades after lung transplantation. FASEB J. 15, 2757–2759.

Poli, M.A., Rivera, V.R., Pitt, M.L., Vogel, P., 1996. Aerosolized specific antibody protects mice from lung injury associated with aerosolized ricin exposure. Toxicon 34, 1037–1044.

Rauber, A., Heard, J., 1985. Castor bean toxicity re-examined: A new perspective. Vet. Hum. Toxicol. 27, 498–502.

Wilhelmsen, C.L., Pitt, M.L., 1996. Lesions of acute inhaled lethal ricin intoxication in rhesus monkeys. Vet. Pathol. 33, 296–302.

Xu, L.L., McVicar, D.W., Ben-Baruch, A., Kunhs, D.B., Johnston, J., Oppenheim, J.J., Wang, J.M., 1995. onocyte chemotactic protein-3 (MCP3) interacts with multiple leukocyte receptors: binding and signaling of MCP3 through shared as well as unique receptors on monocytes and neutrophils. Eur. J. Immunol. 25, 2612–2617.

Zajac-Kaye, M., 2001. Myc oncogene: a key component in cell cycle regulation and its implication for lung cancer. Lung Cancer 34 (Suppl 2), S43–S46.